Nanomechanical Properties of NanoConfined Polystyrene Nanoparticles in Nanoblends

Yahya Rharbi*, M. Yousfi

Laboratoire de Rheologie, UMR 5520
PB 53 Domaine universitaire 38041 Grenoble cedex 9 France
rharbi@ujf-grenoble.fr

Abtract :

The role of nanoconfinement on the glass transition temperature (Tg) of polymers has been extensively studied in the thin film geometry. This work looks at the Tg of nanoconfined polystyrene in spherical nanoparticles (27- 200 nm), individually dispersed in crosslinked polybuthylmethacrylate matrices. A reduction of Tg compared to the bulk was observed in PS nanospheres via neutron scattering-mechanical tests and was found to decrease with decreasing diameter for D< 50nm. The general trend of Tg depression in nanospheres was found to be similar to the results on thin film geometry.

Key-words :

glass transition ; nanomechanics ; polymer nanoblends ; confinement

1   Introduction

The glass transition (Tg) of nanoconfined polymers has been extensively studied throughout the last decade (Rieter (1993) - Riggleman and Al (1997)). The majority of this research has focused on thin film geometry and was carried out on supported and free-standing films using various experimental techniques; Brillouin light scattering, (Forrest and Al (2002)) ellipsometry (Keddie and Al (1994), Kawana and al (2001)), dielectric relaxation (Fukao and Al (2000)), x-ray reflectivity (van Zanten and Al (1996)), fluorescence (Ellison and Al. (2003)). Mechanical measurements on nano-bubble inflation have also been used to probe Tg in ultrathin films (O'Connell and Al (2005)). These reports substantially agreed that the Tg of polystyrene (PS) decreases with decreasing film thickness for h < 50 nm. They demonstrate the relevance of polymer structure and polymer/substrate interactions in confined Tg. Some reports also raised the question of the influence of thin film sample preparation (spin coating) on Tg reduction (Alcoutlabi and Al (2005)). This issue could be settled by studying samples prepared by other means.

Although polymers are often found nanoconfined in geometries such as spheres, little effort has been dedicated to the study of their glass transition. This information could be useful in many industrial and environmental applications; blends, copolymers, nanocomposites, colloids, coatings… One example is zero-VOC coating, which uses polymer nanoparticles in the film-making process (Steward and Al (2000), Tirumkudulu and Al (2005)). VOCs are used in coatings to lower the particle Tg, which permits the fabrication of crack-free films at room temperature. If the Tg is reduced by decreasing the nanoparticle size, the use of VOCs could be avoided, which would have a positive impact on the environment. Another example is in nano-blends, where hard polymer nanoparticles are used to reinforce soft matrices. Reducing nanoparticle size would be counterproductive in this application if it causes the reduction of their Tg. It is therefore of utmost importance to tune in to the study of nano-confined glass transition of polymers in spherical geometries.

This paper describes the influence of the size and the environment of spherical PS nanoparticles, on their glass transition and their nanomechanical properties. It looks at the properties of polystyrene confined in nanospheres (27 nm to 120 nm) within Polybutylmethacrylate (PBMA) matrices. We use a method which combines Nanomechanics with Small Angle Neutron Scattering (SANS) to measure the reduction of the glass transition of PS nanoparticles and we compare these results to those found on thin film geometry. This study also focuses on the effect of proximity of two polymers on their glass transition.

2   Experimental

Polybutylmathacrylate (PBMA) particles (56 nm) and deuterated polystyrene (dPS) particles were prepared using emulsion polymerization, at 70°C for the PBMA and 80°C for the dPS. The polymer concentrations were 10 wt % for the PBMA and 2 wt % for dPS. The PBMA particles were crosslinked at 10% using ethylene glycol dimethylacrylate (EGDMA) during polymerization. The dPS particle size was controlled between 20 and 200 nm by the amount of surfactant SDS in the reaction. The molecular weight measured using GPC was found to be around 400 kg/mol – 600 kg/mol for all the particles investigated here. Particle diameters (D) were measured using dynamic light scattering (Malvern 5000). The bulk glass transition measured by DSC (Perkin-Elmer, DSC7) yielded the following Tg values:

D,nm	27.8	29.8	39.4	52.4	91.2	132.6
Tg,°C	102.2	99.95	99.2	101.9	99.09	99.44

The surfactant and free ions were removed from the dispersions using a mixture of anionic and cationic exchange resins (Dowex, Aldrich). The nano-blends were prepared by mixing dPS and PBMA dispersions to make dPS concentrations of 0.5, 1 and 2 wt % of the solid PBMA. Solid films were obtained after water evaporation at 45 °C.

The small angle neutron scattering (SANS) experiments were carried out on the PAXY instrument at Orphée, Saclay. The scattered neutrons collected on an XY bi-dimensional multi-detector were regrouped according to circular rings to yield spectra of intensities (I) versus the magnitude of the scattering wave vector (q). The range of accessible q values was between 2.3 10^{-3} and 3.4 Å $^{-1}$.

3   Results and discussions

The SANS spectra of films containing up to 2 wt % dPS infer that the dPS nanoparticles are indubitably individually dispersed within the PBMA matrices (FIG.1). The scattering intensity I(q) is the product of the form factor P(q) and the structure facture S(q) of the dPS particles. Up to a volume fraction of 2 %, the structure factor equals 1 and I(q) = P(q). The I(q) intensities were compared to the P(q) of poly-dispersed hard spheres and the diameter and poly-dispersity of the particles were calculated from the best fit. These diameters are similar to those from quasi elastic light scattering (FIG. 1).
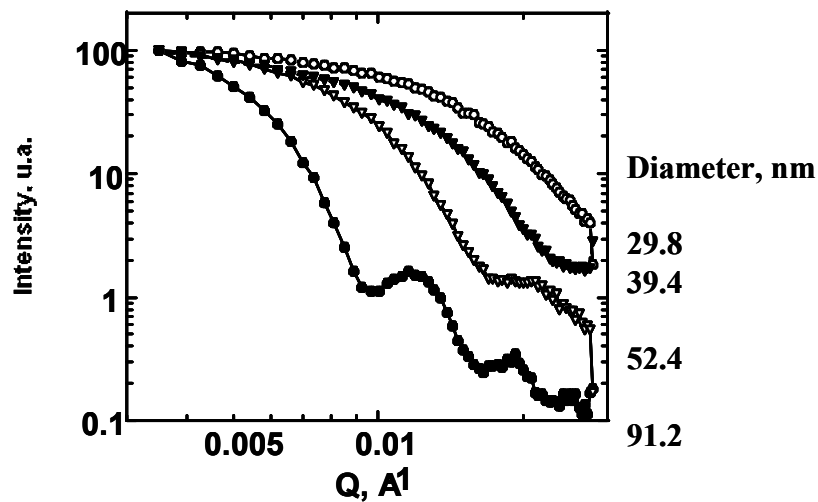
FIG. 1 – Scattering intensities vs. wave vector q for PS nanoparticles dispersed in PBMA matrices.

Films measuring 5×5mm in size and 0.5-1mm thick were compressed in a homemade apparatus in a temperature controlled silicon oil bath by applying a stress of ~4 MPa on the samples for 20s. The samples were then quenched (for about 20s) to room temperature in the deformed state. The total experiment lasted around 60s. During the experiment, the film thickness was reduced to 1/4 of its original size. Because the compressed films were observed with the deformation axis parallel to the neutron beam, the SANS spectra were isotropic. The anisotropy would be seen if the films are visualized with the deformation axis ⊥ to the neutron beam. The scattering intensity of the deformed film was radially averaged and compared to the spectra prior to deformation. At a temperature above Tg of PS, the spectra of deformed films are shifted toward the smaller q values (FIG. 2) and fit the form factor of spherical particles with larger diameters than before deformation. Since the spectra of deformed films below dPS Tg are identical to the non-deformed films (FIG 2), the idea that cavities form around hard dPS particles is discarded.

By assuming dPS nanoparticles deform at a constant volume, one can imagine that they flatten with λ in the compression direction and expand with $\lambda^{1/2}$ in the two other axes. The spectra of the deformed film describe the particle expansion in the two directions perpendicular to the neutron beam. The mathematical form factor of deformed spherical particles, with a deformation axis parallel to the neutron beam was calculated and was found to be exactly equal to the P(q) of a spherical particle with diameter $D = D_0 \lambda^{1/2}$. The deformation rate of individual particles is calculated as $\lambda = (D/D_0)^2$. Figure 3 shows λ vs. [temperature – Tg^{bulk}] for 91.2 nm and 27.8 nm dPS nanoparticles within 10% cross-linked PBMA matrices. The deformation rate (λ) for 91.2 nm dPS particles remains constant and equal to 1 for temperatures below $T^{onset} = 104$ °C, and increases rapidly above this temperature (Fig. 3). The general tendency of λ vs. [temperature – Tg^{bulk}] is the same for all particle sizes, however, the whole nanomechanical curve shifts toward low temperatures as the particle diameter decreases. The 27.8 nm dPS particles begin to deform at a lower temperature ($T^{onset} = 91$ °C) than the 91.2 nm particles. This shift is a clear indication that mechanical behavior of small particles is different from that of large ones. Since the mechanical tests were exactly the same for all particle sizes, the shift of the mechanical curve proves, beyond error, that the glass transition of dPS nanoparticles decreases below bulk value as the particle size decreases.
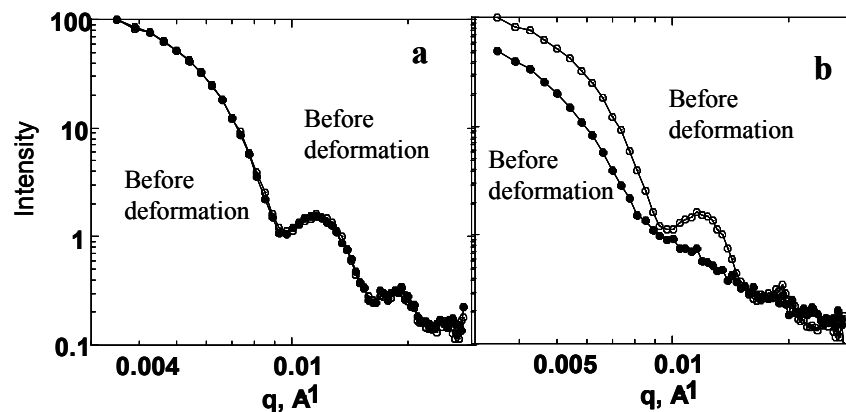
3

FIG. 2 – SANS spectra before and after deformation of 91 nm dPS particles in PBMA matrics .
a) deformed at 65°C and b) deformed at 120°C

The mechanical curves are super-imposable for particle diameters higher than 90nm, which infers that these large particles exhibit a bulk behavior. The temperature shift of the mechanical curve from that of large particles is most likely equal to the deviation of the nanoconfined glass transition (ΔTg) from bulk. Therefore Tg deviation (ΔTg) from bulk is calculated as the temperature shift of the nanomechanical curve of each sample from that of the 130 nm particle. Although the onset temperature of the transition from glassy to rubbery regimes ($T^{onset} = 104\ °C$) is close to $Tg^{bulk} = 99.4\ °C$, for large particles (D > 90 nm), the T^{onset} is not used here as the nanoconfined glass transition.

The contribution of Laplace pressure ($\Delta P = 4\ \gamma_{PS-PBMA}/D$) to particle Tg is negligible; $dTg^{ST} = +\ 0,03\ °K$ for the smallest diameter investigated here. dTg^{ST} is calculated using $\gamma_{PS-PBMA} = 0.72\ mN/m$ and $dTg^{ST}/dP = 0,30°K/MPa$. The Laplace pressure ($dP = 0.1\ MPa$ for 27 nm and 0.02 for 130 nm) could act as a barrier for the deformation of small particles, which could reduce the Tg depression as measured from mechanical tests. However, this is not likely to be the case because the applied stress is larger than the Laplace pressure.
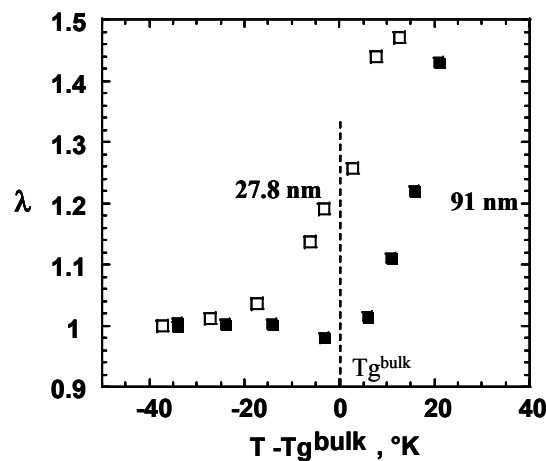

FIG. 3 – Deformation rate (λ) of dPS nanoparticles vs. the deformation [temperature – Tg^{bulk}] for 27.8 nm and 91.2 nm.

4   Conclusions

This report shows the first direct comparison between confinement in thin film geometry and spherical nanoparticles. A shift from bulk Tg (ΔTg) in spherical nanoparticles dispersed in nano-blends was measured. The ΔTg decreases with decreasing particle diameters.

References

Reiter, G. 1993 Mobility of polymers in films thinner than their unperturbed size. *Europhys. Lett*. **23** 579.

Forrest J.A., Dalnoki-Veress K., Stevens J.R. and Dutcher J.R., 1996 *Phys. Rev. Lett.* **77**, 2002.

Keddie J.L., Jones R.A.L and Cory R.A. 1994 Size dependent depression of the glass transition temperature in polymer films. *Europhys. Lett*. **27**, 59.

Fukao K. and Miyamoto Y. 2000 Dielectric and dilatometric studies of glass transitions in thin polymer films. *Phys. Rev. E.* **61**, 1743.

Kawana S. and Jones R.A.L. 2001 Character of the glass transition in thin supported polymer films. *Phys. Rev. E* **63** 021501.

DeMaggio G.B. *and Al*. 1997 Interface and surface effects on the glass transition in thin polystyrene films. 1997, *Phys. Rev. Lett*. **78**, 1524.

Ellison C.J., Kim S.D., Hall D.B. and Torkelson J.M. 2002 Confinement and Processing Effects on Glass Transition Temperature and Physical Aging in Ultrathin Polymer Films: Novel Fluorescence Measurements. *Eur. Phys. J. E* **8**, 155.

Ellison C.J. and Torkelson J.M. 2003 The distribution of glass-transition temperatures in nanoscopically confined glass formers. *Nat. Mater*. **2**, 695.

O'Connell P.A., McKenna G.B. 2006 Dramatic stiffening of ultrathin polymer films in the rubbery regime. *Eur., Phys., J. E*. **20**, 143.

van Zanten J.H., Wallace W.E. and Wu W.L. 1996 Effect of strongly favorable substrate interactions ion the thermal properties of ultrathin polymer films. *Phys. Rev. E* **53**, R2053.

Varnik F., Baschnagel J. and Binder K. 2002 Reduction of the glass transition temperature in polymer films: A molecular-dynamics study. *Phys. Rev. E* **65**, 021507.

Riggleman R.A., Yoshimoto K., Douglas J.F. and dePablo J.J. 2006 Influence of Confinement on the Fragility of Antiplasticized and Pure Polymer Films, *Phys. Rev. Lett*. **97**, 045502.

Alcoutlabi M., and McKeena G.B. 2005 Effects of confinement on material behaviour at the nanometre size scale. *J. Phys.: Condens. Matter* **17**, 461.

Steward P.A., Hern J. and Wilkinson M.C. 2000 An overview of polymer latex film formation and properties. *Adv. Colloid Interface Sci*. **86**, 195.

Tirumkudulu M. S. and Russel W. B. 2005 Cracking in drying latex films. *Langmuir* **21**, 4938.